

Numerical analysis of the liquid ejection due to the gaseous jet impact through computational fluid dynamics

<http://dx.doi.org/10.1590/0370-44672015710079>

Hiuller Castro Araújo

Engenheiro Metalurgista pela
Universidade Federal de Ouro Preto – UFOP
Escola de Minas
Ouro Preto - Minas Gerais - Brasil
hiuller@gmail.com

Eliana Ferreira Rodrigues

Professora
Universidade Federal de Ouro Preto – UFOP
Escola de Minas
Departamento de Engenharia Mecânica
Ouro Preto - Minas Gerais - Brasil
elianafre@em.ufop.br

Elisangela Martins Leal

Professora
Universidade Federal de Ouro Preto – UFOP
Escola de Minas
Departamento de Engenharia Mecânica
Ouro Preto - Minas Gerais - Brasil
elisangelamleal.ufop@gmail.com
elisangelamleal@decat.em.ufop.br

Abstract

Metal droplets generated by an impinging jet, play an important role in metal refining processes, mainly in oxygen steelmaking, where the droplets are ejected into the slag phase. Since the available interfacial area of droplets is very high in this process, the generated droplets enhance the rates of heat transfer and chemical reactions. Therefore, knowledge of the metal droplet generation rate, size distribution and residence time in the slag are of industrial relevance. In this work, the isothermal, transient flow of an incompressible air jet impinging onto an air/water interface at room temperature has been simulated to obtain a better understanding of the droplet ejection phenomenon. The interface was tracked throughout time using the volume of fluid (VOF) technique. The governing equations formulated for mass and momentum conservation and the k- ϵ turbulence model are solved in the axisymmetric computational domain using the commercial code FLUENT. The droplet ejection rates calculated with computational fluid dynamics model are compared to experimental data reported in literature, showing partial agreement, being the incompressibility assumption the probable reason for the deviation observed, which was as far pronounced as the great jet velocity. Nevertheless, the model presented shows itself as a relatively good starting point for the construction of more complex ones (with less simplifying assumptions) which should be able to offer a means to increase the understanding of the droplet ejection phenomena.

keywords: Numerical simulation; computational fluid dynamics; volume of fluid; top blown; droplet ejection.

1. Introduction

The impact of gaseous jets onto gas/liquid interfaces is commonly employed in the metal industry as a way to both stir the liquid phase and introduce chemical species through direct contact between the phases. In the steelmaking industry, the main application of such jets is found in the Linz and Donawitz (LD) oxygen steelmaking process. The oxygen jet is accelerated at supersonic speeds through a convergent-divergent valve and causes the shearing of the metal surface, a phenomenon that is accompanied by the ejection of metal droplets toward the slag (Deo *et al.*, 1996). The formation of the emulsion is primarily responsible for the interfacial area generation required for the reaction

rates needed.

Metal droplets and gas bubbles have a finite residence time in the emulsion and the countercurrent flow of metal droplets and gas bubbles within the emulsion are of relevance to the formation of slag and the kinetics of oxidation/reduction reactions in the converters oxygen (DEO *et al.*, 1996).

According to Geiger *et al.* (1982), the reaction rates that occur in the emulsion metal/slag depends mainly on three factors: (a) the amount of metal in the emulsion metal/slag; (b) the size distribution of the metal drops ejected and (c) the residence time of the droplets in the slag phase. Among the above listed items, the study of metal amount in the emulsion is divided into

two groups: cold experiments, where nitrogen is blown into water at room temperature and hot experiments, which blows nitrogen on molten metal at 1650°C (STANDISH and HE, 1989, 1990; IRONS *et al.*, 2003).

This paper presents a numerical analysis of the droplet ejection phenomenon by means of computational fluid dynamics (CFD) using a mathematical model given by Nguyen and Evans (2006), in order to assess the ability to predict the ejection rates obtained experimentally. A numerical model that has this capability is of great industrial importance as this is a parameter of interest to the oxygen lances design and to improve the reactors of this type.

2. Interaction between jets and liquids

Molloy (1970) investigated the ways of interaction between a gas jet and the surface of a liquid and noted the occurrence of three different behaviors, depending on the gas speed and the distance between the interface and the spear: (a) depression: a jet of lower speed or with a large distance between the lance tip and the surface of the

liquid promotes the formation of a small surface depression (Figure 1a); (b) spreading: a jet of increased speed or a decrease in the distance of the lance tip and the surface promotes the formation of a shallow depression in which is observed a large amount of fluid ejected from the jet (Figure 1b); and (c) penetration: with the continuous increase in

speed or reduction of the distance between lance tip and surface, where there occurs a deep penetration of the jet into the dense phase, with an apparent reduction in the amount of liquid directly scattered by the jet (Figure 1c). Generally, only the last two behaviors are found in pneumatic steelmaking processes (Geiger *et al.*, 1982).

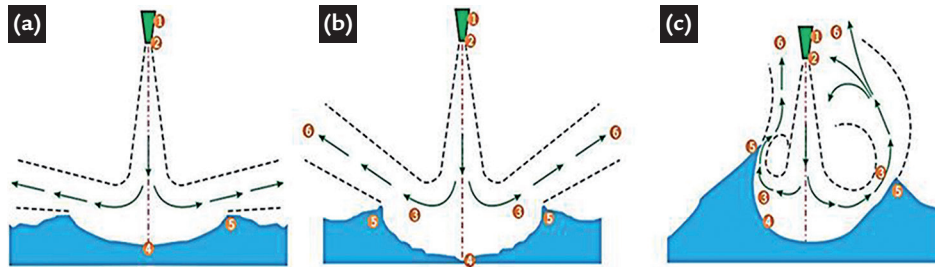


Figure 1
Deformation modes of an interface due to the jet impact: (a) depression; (b) spreading and (c) penetration. Legend: (1) valve; (2) jet exit region; (3) jet along the interface; (4) stagnation point of the original jet; (5) jet separation point along the interface; (6) two-phase flow (adapted from Molloy, 1970).

3. Computational and numerical modeling

As the speed with which the gas leaves the nozzle is relatively high, it is suitable that the flow be simulated using a turbulence model. Turbulent flow fields are characterized by fluctuating speeds. This work uses the k-ε turbulence model. The k-ε model is a

semi-empirical model based on a transport equation model for the turbulent kinetic energy (k) and its dissipation rate (ε). The transport equation for k is derived from the exact equation, while the equation for ε was obtained using physical reasoning and its

exact mathematical counterpart (FLUENT, 2006). These models use the hypothesis of a diffusive gradient relate to the Reynolds tensor, the gradients of the average velocity and the turbulent viscosity, as shown in the following ratio (XIMENES, 2004):

$$\overline{u_i u_j} = -\mu_t \left(\frac{\partial u_i}{\partial x_j} + \frac{\partial u_j}{\partial x_i} \right) + \frac{2}{3} \rho \delta_{ij} k$$

Where: μ_t is the turbulent viscosity and k is the turbulent kinetic energy. The

turbulent kinetic energy (k) and its dissipation rate (ε) are obtained from the

following transport equations (FLUENT, 2006):

$$\frac{\partial}{\partial t} (\rho k) + \frac{\partial}{\partial x_i} (\rho k u_i) = \frac{\partial}{\partial x_i} \left[\left(\mu + \frac{\mu_t}{\sigma_k} \right) \frac{\partial k}{\partial x_j} \right] + G_k + S_k$$

$$\frac{\partial}{\partial t} (\rho \epsilon) + \frac{\partial}{\partial x_i} (\rho \epsilon u_i) = \frac{\partial}{\partial x_j} \left[\left(\mu + \frac{\mu_t}{\sigma_\epsilon} \right) \frac{\partial \epsilon}{\partial x_j} \right] + C_{1\epsilon} \frac{\epsilon}{k} G_k - C_{2\epsilon} \rho \frac{\epsilon^2}{k} + S_\epsilon$$

In these equations, G_k represents the turbulent kinetic energy generation due to the speed gradients; $C_{1\epsilon}$ and $C_{2\epsilon}$ are constants; σ_k and σ_ϵ are turbulent Prandtl numbers for k and ε, respec-

tively; and S_k and S_ϵ are the source terms of k and ε, respectively. The constants of the k-ε turbulence model, $C_{1\epsilon}$, $C_{2\epsilon}$, C_{μ} , σ_k and σ_ϵ have the standard values of 1.44; 1.92; 0.09; 1.0; and 1.3,

respectively. A complete discussion of the turbulence model k-ε can be seen in Wilcox (1994). The properties of the fluids used in the numerical model are shown in Table 1.

Property	Liquid water	Air
Specific mass [kg/m ³]	998.20001	1.225
Specific heat [J/kg.K]	4182.00	1006.43
Thermal Conductivity [W/m.K]	0.60	0.0242
Dynamic Viscosity [kg/m.s]	0.0010003	1.7894 × 10 ⁻⁵
Molecular Mass [kg/kmol]	18.0152	28.966
Characteristic distance of L-J * [10 ⁻¹⁰ m]	0	3.711
Energy parameter of L-J [K]	0	78.6
Thermal expansion coefficient [1/K]	0	0

Table 1
Values of the properties of the fluids used in the numerical model.

4. Results and discussion

Six computer simulations were carried out, where the jet speeds were varied for the computational domain (u_{in}). The problem was numerically simulated for speeds ranging from 56.2 to 116.2 m/s, steps of 10 m/s. Thus, it was possible to evaluate the liquid ejection rates corresponding to Weber numbers ranging between 4.5 and 19.3.

The observation of the interaction modes between gas stream and liquid pool can be made by means of volumetric fraction contour plots in order to evaluate the instantaneous distribution of the phases in the computational domain. Figure 2 shows

a contour map obtained for two different input speeds. In this figure, for the lower speed, it is noticed that a diffused region can be identified on the edge of the cavity produced by the jet, suggesting that there exists a spray of water. The presence of the spray corresponds to the way indicated in Figure 1a, the generation of droplets observed by Standish and He (1989), characteristic of moderate gas flow and/or large heights lance. As for the higher speed, the interaction mode described by Molloy (1970) as penetration mode (Figure 1c) is observed. This result confirms that the increase in jet speed in the com-

putational domain leads to the increase in the interaction between the jet and the bath, and a much larger amount of water suspended on the liquid pool.

In addition to promoting the liquid droplets ejection, the jet impact induces the movement of the liquid. Figure 3 shows the velocity field of the liquid phase obtained by numerical simulation for an input speed of 66.2 m/s. In this figure, one can observe the formation of vortices in the liquid phase in the anti-clockwise around the axis of symmetry, where the velocity vectors in the liquid phase are expressed in m/s and colored by velocity magnitude.

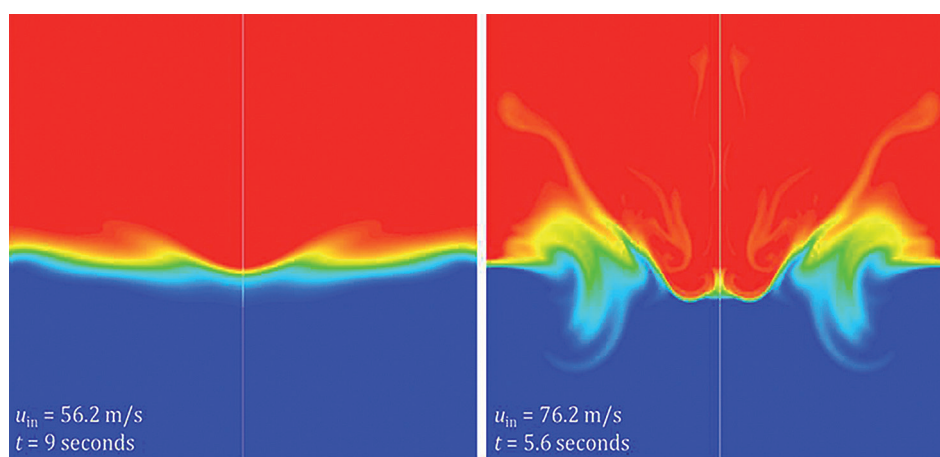


Figure 2
Volume fraction contour map (phase water in blue) in the computer simulation at different time.

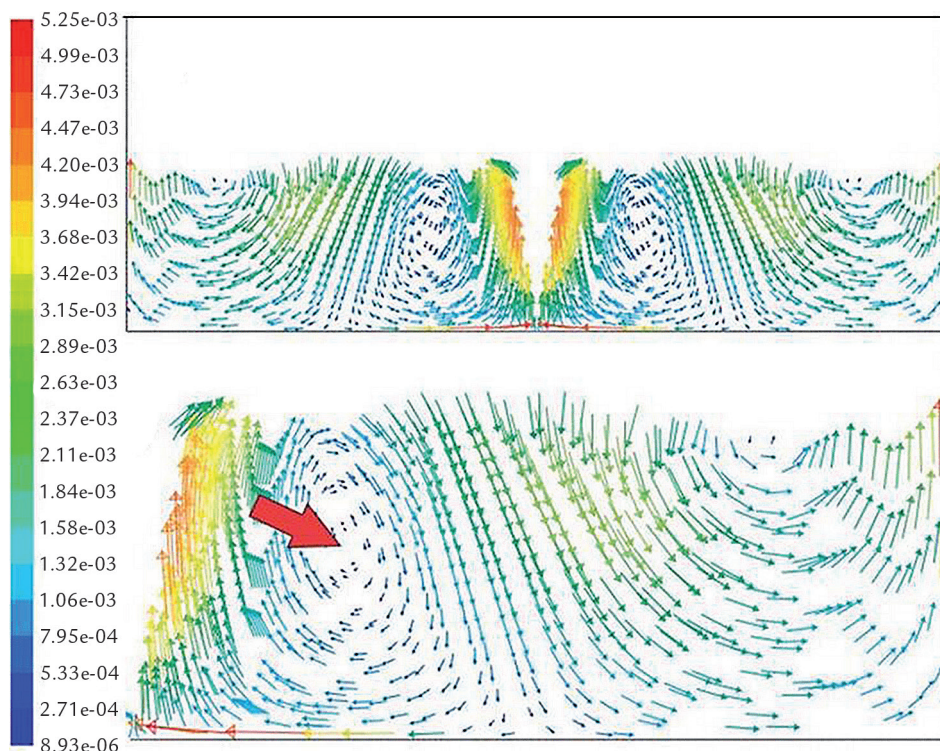


Figure 3
(a) Velocity field in the liquid phase to 66.2 m/s. (b) the right portion showing a vortex in the liquid phase induced by the jet.

Figure 4 shows the volume fraction map (index a) and the corresponding velocity fields (index b) for the time simulation of 1 second. The volume fraction is

in the left and the velocity field is in the right. In all simulations, it was observed that the primary impact (the first moment of blowing), the jet moves radially large

amount of water, while for higher speeds the bottom of the computational domain was reached. This phenomenon can be observed by analyzing the history of the

depth of the cavity. In the case of higher jet velocity, a lower spreading liquid is observed. This apparent nonsense can be resolved by the associated velocity field analysis, which clearly shows that at the time of 1 second, blowing is at a more advanced stage of evolution, since the liquid deflected radially towards the

vertical walls of the model is already offset toward the pool.

Figure 5 shows the variation of impact cavity calculated by CFD model over the simulation time with the input speed of 86.2 m/s. Note the great disturbance in the early stages, denoted by large amplitude of oscillation followed

by damping and then the tendency of the cavity depth oscillates around an equilibrium value. These observations confirm the interpretations of Nguyen and Evans (2006) that, in general, the simulation of the impact of the gas jet in a liquid/gas interface reaches a quasi-steady state within the first 10 seconds.

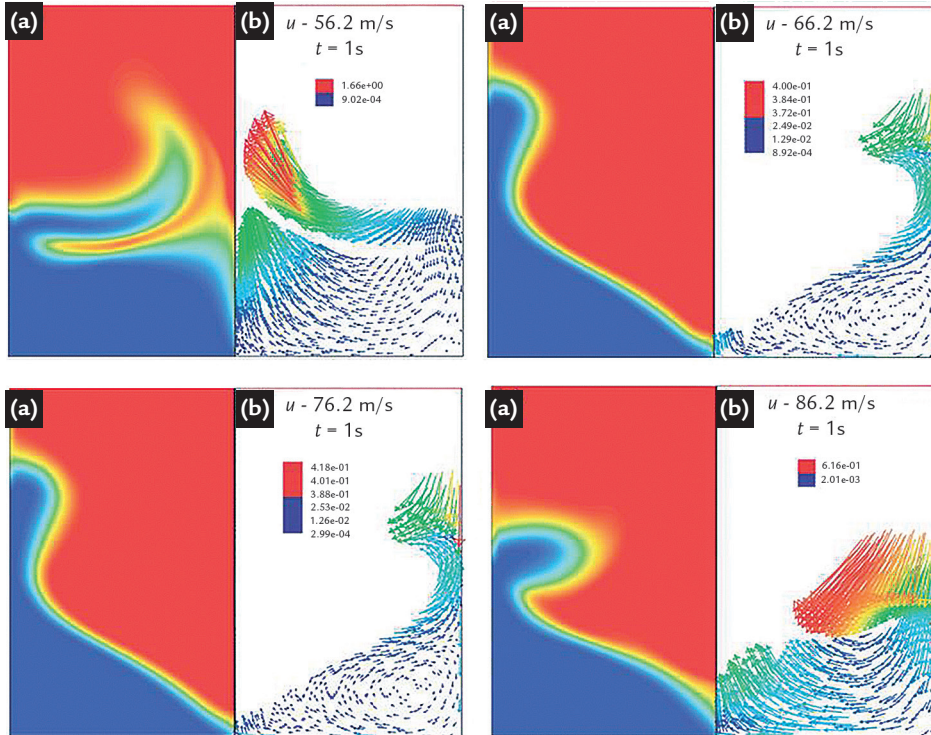


Figure 4
Graph represents (a) a volume fraction map to different input velocities and (b) the velocity field in the cells that satisfy the condition $0.6 \leq \phi_{\text{water}} \leq 1.0$.

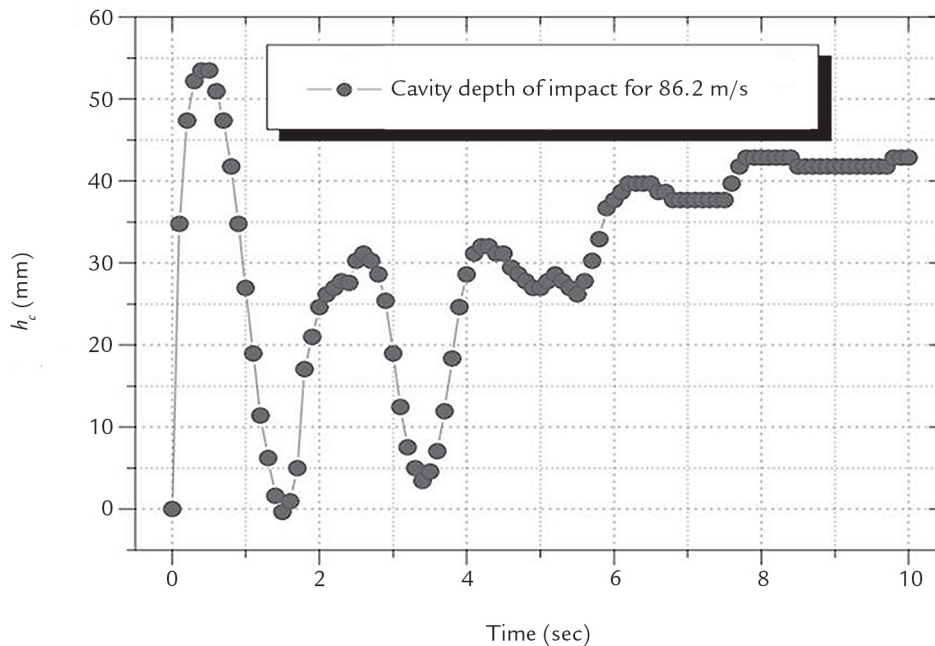


Figure 5
Time variation of the cavity depth generated by the gaseous jet impact.

5. Conclusions

In this work, the results of transient and isothermal (25°C) numerical simulations in two dimensions of the impact of the air jet in the air/water interface were presented. The simulations were compared to

both experimental data of ejection rates and models of the depth of the cavity generated by the impact provided by literature. Simplifying assumptions were adopted for the numerical modeling; that is, the gas phase

was considered to be incompressible and the flow was considered to be isothermal.

The analysis of contour maps of volumetric fraction showed that the computer model was able to exhibit the

ways of generating droplets comparable to those observed in the physical modeling using a high speed cinematography technique (Standish and He, 1989). The results led also to observe the change in the intensity of the interaction jet / liquid pool with increasing jet speed in the com-

putational domain.

A comparison of the ejection rates calculated by the model with those reported in the literature showed partial agreement, with deviations ranging from about 30 to 50%. This hypothesis should, however, be verified by conducting a new

set of simulations, taking the energy equation and the compressibility of the gaseous phase into consideration. The predicted depth of the impact cavity proved to be very efficient. This result agrees with those obtained by simulation of the same physical situation (Nguyen and Evans, 2006).

Acknowledgments

The authors acknowledge the Brazilian Federal University of Ouro

Preto (UFOP) and those who helped in the execution of this project.

References

- DEO, BRAHMA *et al.* Characterization of slag metal droplet gas emulsion in oxygen steelmaking converters. *ISIJ International*, v. 36, n. 6, p. 658–666, 1996.
- FLUENT. FLUENT 6.3 User's Guide. Lebanon, 2006.
- GEIGER, GORDON H. *et al.* BOF steelmaking volume one introduction, theory and design. Warren dale: Iron and Steel Society of the American Institute of Mining, *Metallurgical and Petroleum Engineers*, 1982. cap. Paul V. Chapter Five Theory of B.O.F. Reaction Rates, p. 612.
- IRONS, GORDON *et al.* Generation of droplets in slag metal emulsions through top gas blowing. *ISIJ International*, v. 43, n. 7, p. 983–989, 2003.
- MOLLOY, N. A. Impinging jet flow in a two phase system: the basic flow pattern. *Journal of the Iron and Steel Institute*, v. 208, n. 10, p. 943–950, 1970.
- NGUYEN, AHN V. EVANS, GEOFFREY M. Computational fluid dynamics modeling of gas jets impinging onto liquid pools. *Applied Mathematical Modeling*, v. 30, p. 1472–1484, 2006.
- STANDISH, NICHOLAS, HE, QING LIN. Drop generation due to an impinging jet and the effect of bottom blowing in the steelmaking vessel. *ISIJ International*, v. 29, n. 6, p.455–461, 1989.
- STANDISH, NICHOLAS, HE, QING LIN. A model study of droplet generation in the b.o.f. steelmaking. *ISIJ International*, v. 30, n. 4, p. 305–309, 1990.
- WILCOX, DAVID C. *Turbulence modeling for CFD*. (2nd printing-with corrections). La Canada: DCW Industries, 1994. 460 p.
- XIMENES, CLEBER SANDIM. *Aplicação de técnicas de fluidodinâmica computacional (CFD) em fornos para produção de cimento*. Campinas: UNICAMP, 2004.

Received: 15 May 2015 - Accepted: 3 June 2017.